JOURNAL OF MATERIALS SCIENCE 29 (1994) 4086–4092

The evaluation of hot-working characteristics of cobalt-based implant alloys

JONG-CHENG TSAI, JING-BANG DUH, SHAN-CHANG CHUEH
Materials Research Laboratories, Industrial Technology Research Institute, Chutung, Hsinchu, Taiwan 310

The hot-working characteristics of wrought Co–Ni–Cr–Mo implant alloy during ingot-to-billet conversion were evaluated using a Gleeble-2000A simulator. The hot tensile test at 700–1320 °C was used to determine the optimum hot-working parameters at a strain rate equivalent to that of conventional press forging to ensure acceptable hot workability. Hot ductility and deformation resistance as a function of temperature can be clearly established. The fracture surfaces of the tensile specimens were examined to correlate them with the hot tensile ductility values at various temperatures. The poor ductility at temperatures above 1300 °C was attributed to the incipient melting of grain boundaries. The effect of temperature and strain rate on the flow-stress behaviour and microstructures were investigated by uniaxial compression testing in the temperature range 900–1200 °C and strain rate, $\dot{\varepsilon}$, range of 0.01–10 s^{-1}. The strain-hardening and steady-state behaviour were described from the measured true stress–true strain curves.

1. Introduction

High-strength cobalt–nickel multiphase (MP) alloy, originally developed by Smith [1], possessed a profound combination of properties, namely, high strength, and excellent corrosion resistance [2–4], and is well qualified for aerospace application at elevated temperatures. Later, the wrought Co–Ni–Cr–Mo alloy (MP35N) was evaluated in the Suzler Research and Development Laboratory as a substitute for 316L stainless steel and cast Co–Cr–Mo alloy for surgical implant application [5], because this wrought Co–Ni–Cr–Mo alloy exhibits ultra-high strength and improved fatigue strength, which effectively would reduce the possibilities of failure found in cast cobalt alloy [6]. Despite the relatively high material cost, the Co–Ni–Cr–Mo alloy offers great potentials for application in surgical implants and is now highly noticed and even commonly used. The Co–Ni–Cr–Mo alloy with higher nickel content (35% Ni) was developed to increase stacking fault energy and would demonstrate better forgeability [7]. A low stacking fault energy is often considered a detriment to hot workability, due to the inhibition of the recovery process resulting from difficulty of cross-slip [8]. In the actual rolling practice of this alloy, it was reported that wedge cracks were observed even with moderate reduction [9]. The poor workability and high deformation resistance of Co–Ni–Cr–Mo alloy in the cast ingot state can be attributed to the non-uniform grain structures, shrinkages and impurity segregation after the initial melting practice. Therefore, if this high-strength cobalt as-cast alloy was subjected to close-die forging for artificial implants fabrication, a secondary remelting process, prior to forging, is strongly recommended. In this study, the electroslag remelting (ESR) technique was used to improve the hot workability of this material. Conventionally, the remelting practice of vacuum-arc remelting was adapted [10]. The ESR process can significantly render homogeneous structure and reduce segregation and detrimental trace elements, such as sulphur, which would impair the forgeability [11, 12]. Breakdown of Co–Ni–Cr–Mo alloy ingot requires careful control of processing parameters, otherwise, various kinds of metallurgical defects will occur. In previous studies on wrought Co–Ni–Cr–Mo alloy, efforts were mostly aimed at the strengthening mechanism at room temperature [10, 13, 14] and phase transformation during ageing treatment [15, 16]. Limited research has focused upon the hot-working characteristics of this alloy [17]. In fact, definition of the hot-working temperature range is the essential step in setting up a good hot-working procedure, especially for a poor ingot structure. The main purpose of this work was to determine the hot-working parameters during ingot-to-billet conversion by Gleeble-2000A simulator. Hot tensile tests were employed to realize the hot ductility and deformation resistance as a function of temperature, tested at the strain rate equivalent to that of press forging. Therefore, the optimum preheat temperature and working temperature range can be clearly established. The flow stress deformed at various strain rates and temperatures is measured by a hot compression test, which can predict the desired mechanical capacity as the alloy is hot worked at different types of forming processes.

0022–2461

2. Experimental procedure

The Co–Ni–Cr–Mo alloy was first melted as an electrode in an air-induction melting furnace equipped with a bottom plug for argon blowing. The cast alloy was remelted with a 30 kg laboratory scale electroslag remelting furnace. The electrode was 70 mm diameter and the inner diameter of the water-cooling copper mould was 120 mm. Its nominal composition (wt %) was Co–20Cr–10Mo–36Ni–0.02C.

The hot-working behaviour was investigated in a thermal-mechanical servo controlled 8 ton Gleeble-2000A tester. The test machine was used to obtain the ductility and strength at elevated temperatures ranging from 700–1320 °C by hot tensile testing. Tensile specimens were prepared with 10 mm diameter and 120 mm length, which were held horizontally by stainless steel jaws in the test chamber. The temperature of the specimen was monitored and controlled by a thermocouple percussion-welded to the specimen surface at its midlength. Electric power was introduced to resistance heat the specimen under the desired heating cycle that simulated a practical hot-working sequence. Two types of tensile test were employed to determine the optimum hot-working parameters [18]:

(i) on-heating: specimens were heated to the test temperatures in 60 s and then pulled in tension to fracture at a constant strain rate of 1.0 s^{-1};

(ii) on-cooling: unmachined specimen blanks were heated in a furnace at a given preheat temperature (determined from the on-heating test) for 2 h and then water-quenched. After machining, specimens were reheated to the preheat temperature in the Gleeble-2000A unit for 60 s to dissolve any phases which may have precipitated, and held for 60 s, then cooled to the test temperature at 2.5 °C s^{-1} and held for 30 s, and finally pulled at the same strain rate as in the on-heating test.

Hot ductility was evaluated from the reduction of area upon rupture and the hot strength by the maximum tensile strength. The fracture surfaces of tensile-test specimens were examined by scanning electronic microscopy (SEM), to observe the fracture mode.

Cylindrical specimens, 10 mm diameter and 12 mm high, were machined for the hot compression test. The end surfaces were grounded parallel. Graphite foil was used as lubricant to reduce friction between the flat tungsten dies and the specimen. The specimens were directly heated to the test temperature, soaked at that temperature for 60 s, and compressed to a true strain of 0.5. Once the compression was finished, the specimens were water-quenched to retain the high-temperature structure. The retained microstructure was examined by optical microscopy. The etchant with 2 parts HCl and 1 part HNO_3 was used. Both the temperature and strain were kept constant during compression. The true stress–true strain curves were measured by attaching a diametrical strain gauge at the midlength of the specimen. Hot compression tests were conducted in the temperature range 900–1200 °C and in the strain-rate range of 0.01–100 s^{-1}, which were analysed to obtain the temperature and strain-rate dependence of the flow stress of cast Co–Ni–Cr–Mo alloy. These strain rates covered those used in conventional rolling, extrusion and forging practices.

3. Results and discussion

The principal advantage of the hot tensile test for metalworking process is that it can clearly establish the optimum maximum and minimum hot-working temperature [12]. The per cent reduction of area (RA) is the primary result to assess the ability of the material to withstand crack propagation during hot deformation [19]. The ultimate tensile strength and the hot ductility of various test temperatures by an on-heating tensile test at the strain rate of 1.0 s^{-1} are shown in Fig. 1a and b. The ultimate tensile strength decreases as the temperature increases from 700 °C to 1320 °C. The strength is less than 200 MPa above 1200 °C, but the strength is approximately doubled at 900 °C and its dependence on temperature below 900 °C is very pronounced. At temperatures higher than 1300 °C, the 0.2% yield strength was not measurable and the ultimate tensile strength was less than 100 MPa. This meant that the alloy almost lost its hot strength above 1300 °C.

The alloy exhibits good hot ductility (RA > 50%) for a wide range of temperatures from 800–1200 °C as demonstrated in Fig. 1b. Experience has indicated that a general qualitative rating scale between reduction of area and hot workability could be given to define

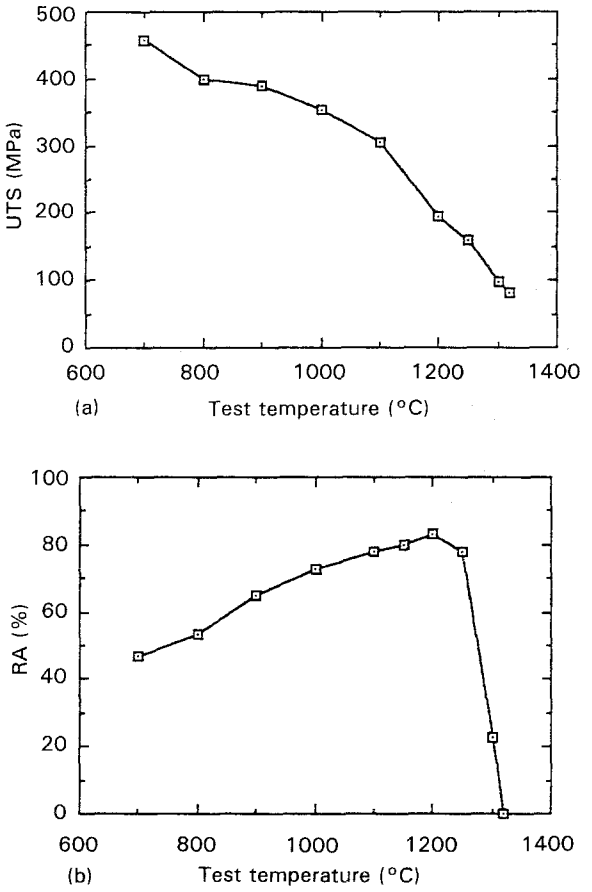

Figure 1 Temperature dependence of hot tensile properties tested at $\dot{\varepsilon} = 1.0\ s^{-1}$ by the on-heating mode: (a) ultimate tensile strength, (b) hot ductility.

suitable hot-working parameters [12]. These ratings can be used to determine the hot-working temperature range and the allowable deformation amount. The maximum permissible deformation per pass for hot working of this cobalt alloy at different temperatures, which is obtained directly proportional to reduction of area, are shown in Fig. 1b. A normal deformation amount is suggested when the reduction of area exceeds 50%, but a smaller deformation is necessary when ductility is below this value [12]. Nevertheless, the surfaces of as-cast workpieces are rather rough, surface cracks are easily initiated and propagated; therefore, the allowable amount of deformation should be more conservative. In addition, according to this rating system, 800 °C is designed as the minimum hot-working temperature in Fig. 1b, because at 800 °C the reduction of area begins to fall below 50%. The peak ductility occurs at 1200 °C and drops rapidly above 1300 °C. The peak ductility temperature (PDT) is determined to be 1200 °C and the zero ductility temperature (ZDT) is 1320 °C; the optimum preheat temperature lies between PDT and ZDT [12]. For this cast cobalt-based alloy, the preheat temperature is selected as between 1200 and 1250 °C for the subsequent on-cooling test. The on-cooling tensile test is used to realize how closely the ZDT can be approached before the hot ductility is severely reduced.

Fig. 2a and b shows the on-cooling tensile results obtained from the specimens which have been preheated at 1200 and 1250 °C for 2 h in the furnace and tested by the on-cooling mode. The on-cooling ductility and strength level for each preheat, at hot-working temperatures, are also strongly dependent upon temperature, as shown in Fig. 1. The hot-strength value in Fig. 2a demonstrates that the deformation resistance does not vary with the preheat temperature to the same degree as does ductility in Fig. 2b. In addition, the strength measured in the "on-cooling" scheme is lower than that measured in "on-heating" tests. The hot ductility of Co–Ni–Cr–Mo alloy ingot determined from both on-heating and on-cooling tensile tests is presented in Fig. 3. It is clearly recognized that the effect of thermal history on the hot ductility of the alloy is evident. The highest hot ductility can be obtained from the 1250 °C preheating at test temperatures of 800–1250 °C, somewhat lower at 1200 °C and the lowest value occurred at the on-heating condition. The optimum preheat temperature is 1250 °C, because it provides a good hot ductility level from 800–1250 °C. A microstructural examination between on-heating and on-cooling tests was used to interpret the ductility and strength variation (Fig. 4). The specimen used for on-heating tensile tests shows a typical as-cast dendritic structure of a strong cored cobalt f c c matrix as in Fig. 4a. After preheating at 1200 and 1250 °C for 2 h, the dendritic structure tends to diminish and be homogenized as shown in Fig. 4b and c. Annealing twins are also clearly observed within the grains. The grain size on preheating at 1200 and 1250 °C is 50 and 150 μm, respectively. The coarser grains occur at the higher preheat temperature of 1250 °C in Fig. 4c, which will restrict the grain-boundary sliding, because the alloy is hot worked

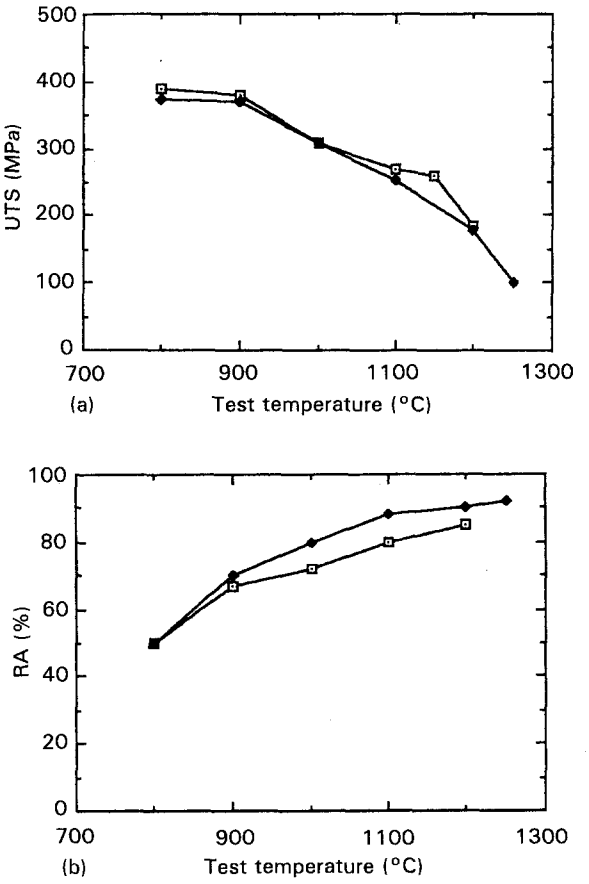

Figure 2 Temperature dependence of hot tensile properties tested at $\dot{\varepsilon} = 1.0\,s^{-1}$ by the on-cooling mode preheated at (⊡) 1200 °C, (◆) 1250 °C. (a) ultimate tensile strength, (b) hot ductility.

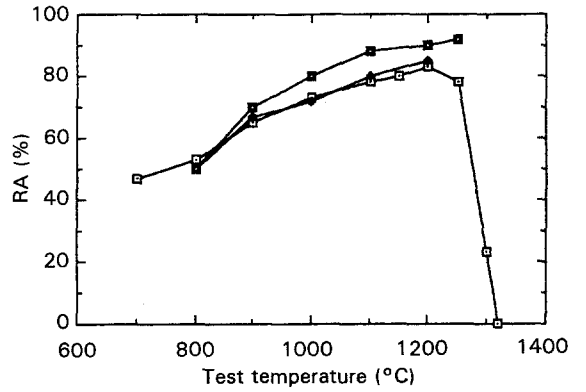

Figure 3 The effect of thermal history on the hot ductility of ESR Co–Ni–Cr–Mo alloy. (⊡) on-heating; (◆) 1200 °C preheat, on-cooling; (■) 1250 °C preheat, on-cooling.

at elevated temperature. Hence, the hot ductility of 1250 °C preheating is greater than that of 1200 °C. Through an appropriate preheating treatment, higher hot ductility can be achieved by producing a homogeneous grain microstructure. Nevertheless, it is wise to avoid preheating the alloy close to the ZDT in industrial practice, because the interior region of the workpiece may not cool sufficiently from near ZDT to achieve good hot ductility, thereby bringing about extensive centrebursting defects during hot working, as seen in Fig. 5. In addition, the minimum hot-

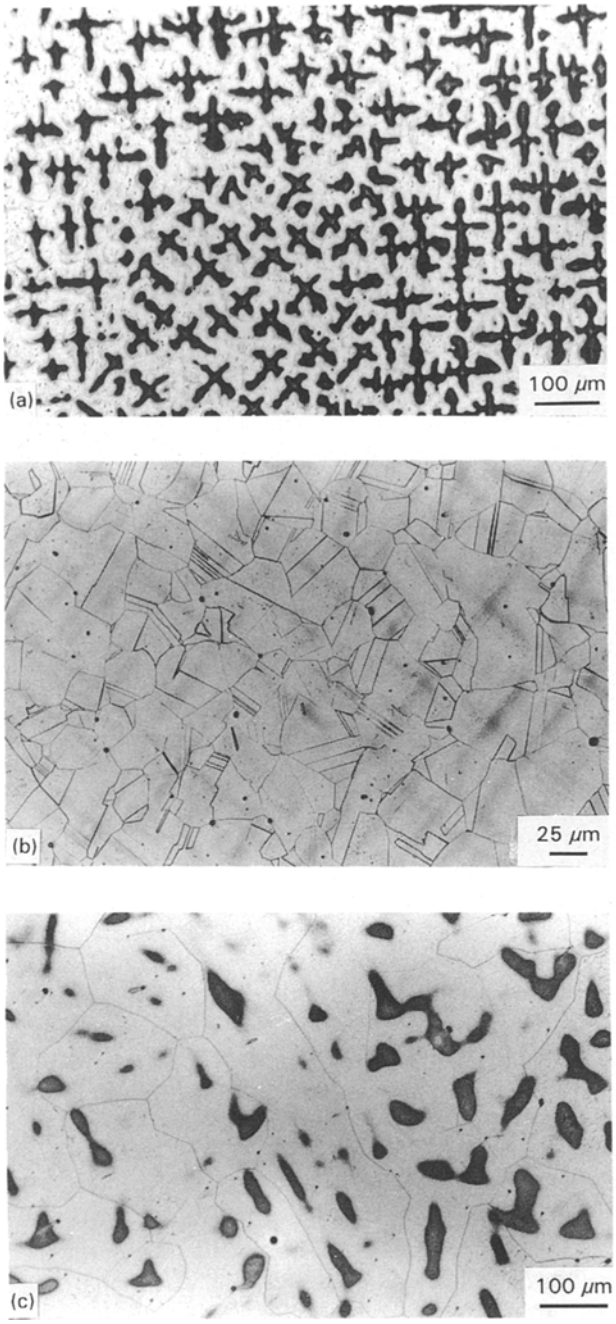

Figure 4 The effect of preheat treatment on microstructure: (a) as-cast, (b) 2 h at 1200 °C, (c) 2 h at 1250 °C.

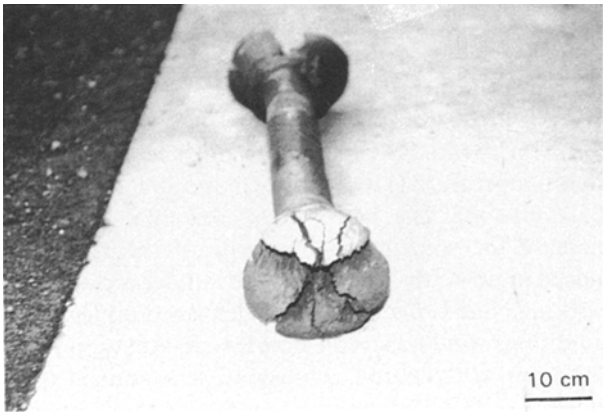

Figure 5 Centreburst of the ingot forged at 1275 °C.

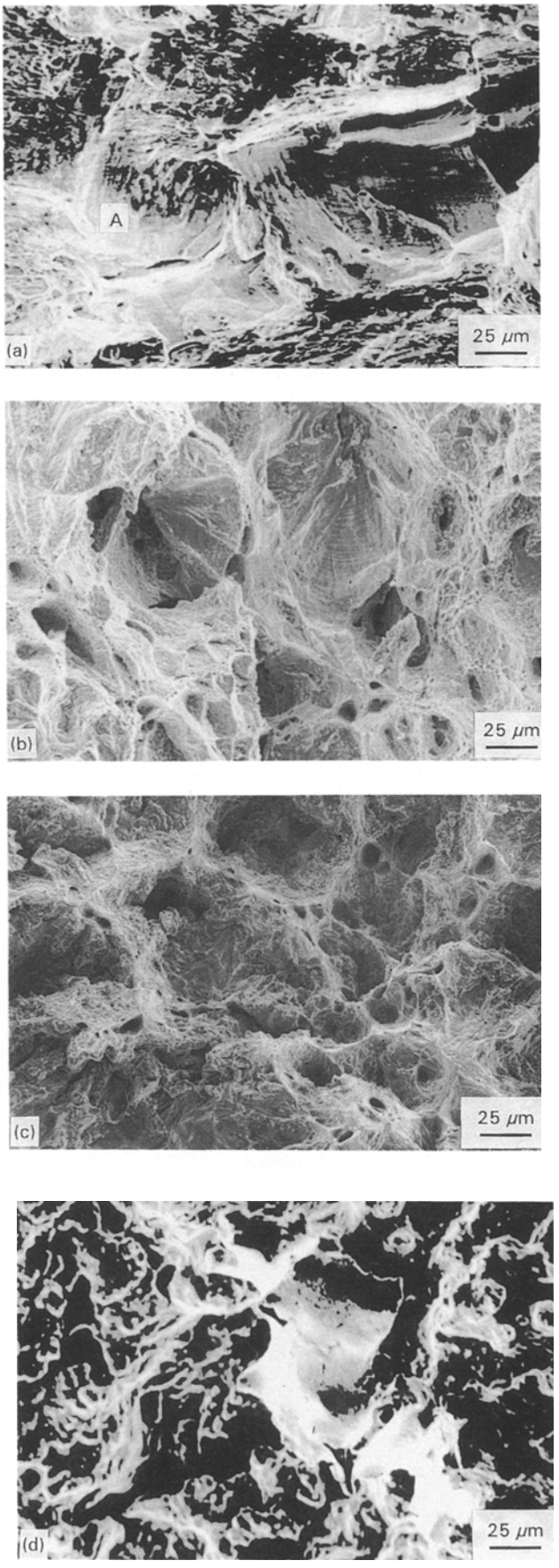

Figure 6 Scanning electron micrograph of fracture surfaces tensile tested at (a) 800 °C, (b) 1100 °C, (c) 1200 °C, (d) 1300 °C.

working temperature is determined as 800 °C in the press-forging process for acceptable hot ductility above 800 °C. There are only a few small surface cracks found in subsequent practical forging parts.

The fracture surface of a tensile specimen at 800 °C exhibits large transgranular cleavage, such as at A; elsewhere the surface contains some small and shallow dimples in Fig. 6a. The scanning electron micrograph in Fig. 6a reveals that the fracture mode at 800 °C is predominantly ductile but partially brittle. At a temperature higher than 1100 °C, the appearance of fractography is similar to that observed above, but the number of small dimples increased (Fig. 6b), indicating that the alloy will become more ductile with increasing temperature. As the temperature increases to 1200 °C, the local transgranular cleavage facets seen in Fig. 6a and b disappear (Fig. 6c). Total dimple fracture is typical of relative ductile rupture, confirming the superior reduction of area obtained at this temperature. Once the temperature reaches 1300 °C, the main fracture path is intergranular, and the incipient melting of the grain boundary is visible locally in Fig. 6d, which accounts for the drop-off in hot ductility. Fracture at ZDT (1320 °C) is essentially intergranular, which is facilitated by the incipient melting at grain boundaries in Fig. 7a. The intergranular crack along the grain boundary is more obvious in Fig. 7b. The weakness of the grain boundary significantly induces the brittleness of the Co–Ni–Cr–Mo alloy deformed at extremely high temperature. Microstructural evidence of incipient melting at the ZDT has also been detected in nickel-based superalloy [12], Inconel 600 superalloy [20] and Ti–6Al–4V alloy [21]. In this study, the poor hot ductility at temperatures above 1300 °C is mainly attributed to the incipient melting of grain boundaries.

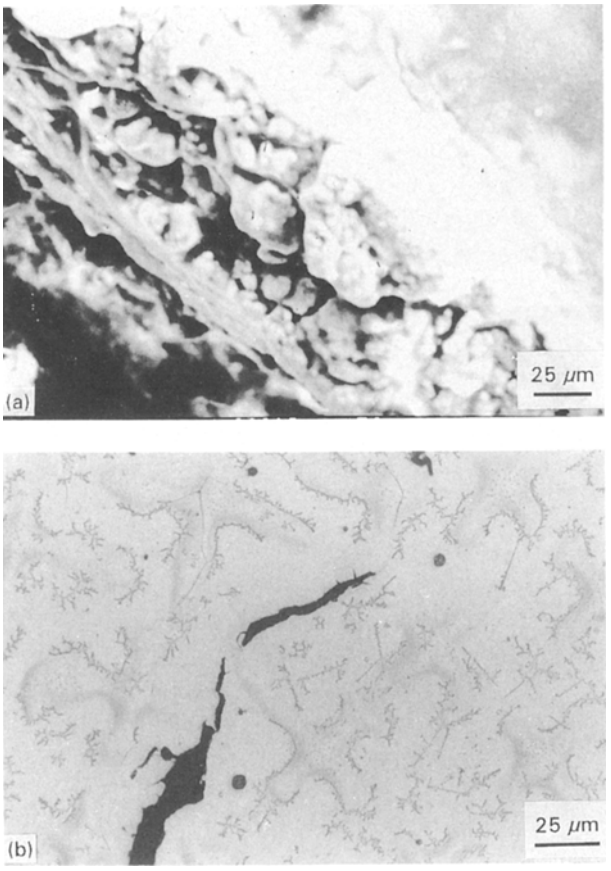

Figure 7 (a) incipient melting of a grain boundary pulled at 1320 °C; (b) optical micrograph of an intergranular crack due to the incipient melting at 1320 °C.

The true stress–true strain curves measured at 900–1200 °C at different strain rates by the hot compression test are presented in Fig. 8a–d. The measured flow stress (Fig. 8) shows a strong dependence on strain rate and temperature – the flow stress increases rapidly with increasing strain rate and decreasing temperature. The dependence is similar to that found in the hot working of cast Co–Cr–Mo alloy [8, 22]. The alloy shows strain-hardening characteristics at all strain rates at 900 °C in Fig. 8a. Strain hardening is particularly evident at the high strain rate of 10.0 s^{-1}, and raises significantly the stress level. However, there is not much stress difference at the strain rate of 0.01–1.0 s^{-1} beyond 0.2 strain. The plastic flow shows a similar strain-hardening phenomenon when compressed at 1000 °C in Fig. 8b, but a decreasing rate of strain hardening at a lower strain rate of 0.01 s^{-1} is seen in Fig. 8b. At the higher temperature of 1100 °C, a significant steady-state deformation behaviour, in which the strain hardening is in equilibrium with a dynamic restoration process [23], occurs at the lowest strain rate of 0.01 s^{-1} just at very small strain in Fig. 8c. The steady-state flow will approach as the flow-softening process rapidly balances the strain-hardening process, i.e. the flow stress remains invariant with strain and time. The behaviour of steady-state flow can only be achieved under hot deformation at a certain temperature and strain rate [24–27]. In the strain-rate range from 0.1–10 s^{-1} at 1100 °C, the curves are characteristic of dynamic recrystallization during hot working [28], and exhibit a hump at intermediate strains and flow softening at large strain. Upon further increasing the temperature to 1200 °C, the behaviour of flow stress in Fig. 8d is quite similar to that observed as above in Fig. 8c. The strain rate at which the alloy starts to exhibit steady-state flow shifts to higher values with increasing temperature. A steady-state flow is more easily reached at high temperature than at low temperature, even at small strain, because the diffusional process and thermally activated dislocation movement are enhanced at high temperature.

The effects of strain rate on the flow-stress behaviour are also indicated in Fig. 8. At low strain rates of 0.01 and 0.1 s^{-1}, the material exhibits steady-state flow above 1100 °C in Fig. 8c and above 1200 °C in Fig. 8d, respectively. However, as the strain rate increased above 1.0 s^{-1}, steady-state flow behaviour is absent at all temperatures in Fig. 8a–d. These curves indicate that the steady-state deformation of the cast Co–Ni–Cr–Mo ESR alloys can only be achieved at high temperature (1100–1200 °C) and low strain rate (0.01–0.1 s^{-1}). The addition of elemental nickel to increase the stacking fault energy of the alloy did indeed improve the hot workability under certain hot-working conditions. The alloys deformed under these conditions would also consume less deformation load.

The microstructural changes were examined as a function of hot compression parameters to investigate the behaviour of the stress–strain curves of Fig. 8. The

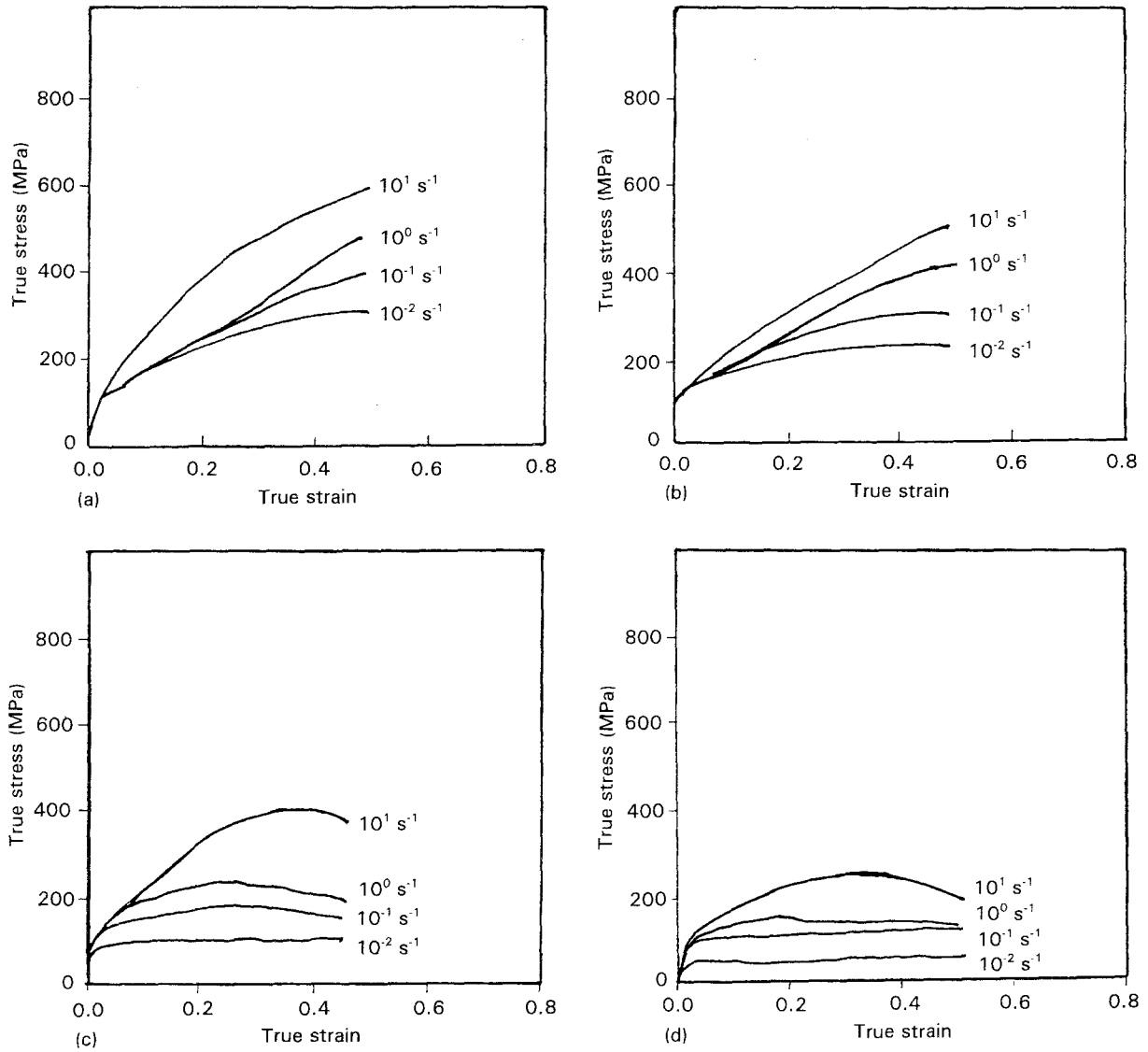

Figure 8 True stress–true strain curves for various test temperatures at strain rates of 0.01–10 s^{-1}: (a) 900 °C, (b) 1000 °C, (c) 1100 °C, (d) 1200 °C.

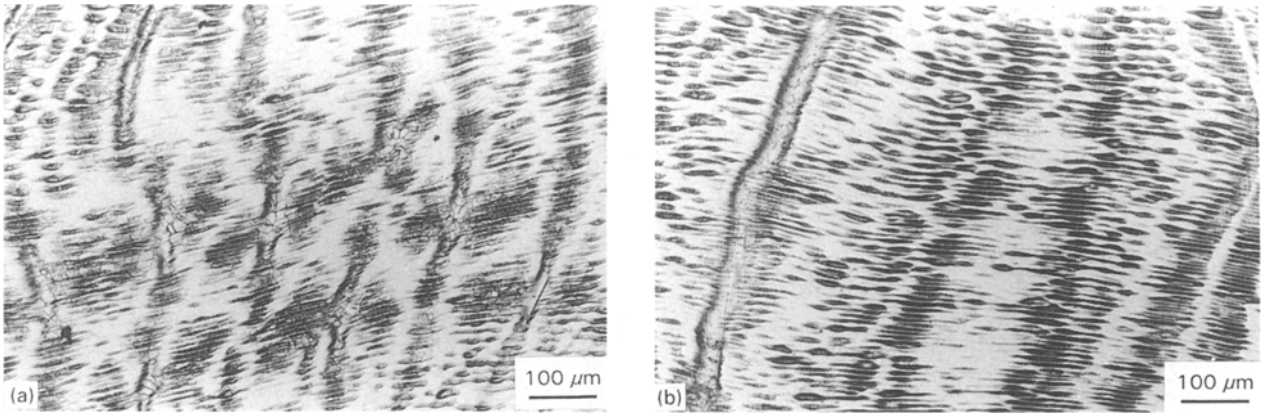

Figure 9 The effect of strain rate on the plastic flow at 1200 °C: (a) 0.01 s^{-1}, (b) 10 s^{-1}.

original as-cast microstructure is still retained after compression at 1200 °C for strain rates of 0.01 and 10.0 s^{-1}, as shown in Fig. 9a and b. At a higher strain rate of 10.0 s^{-1}, there is strong evidence of flow localization along intense shear bands associated with the dendritic core. Some recrystallized grains are formed locally, where the strains are large. This would indicate that the primary flow-softening mechanism in Fig. 8d is due to dynamic recrystallization. The behaviour is consistent with the low value of stacking-fault energy for this alloy. The plastic flow is more homogeneous at a lower strain rate of 0.01 s^{-1} in

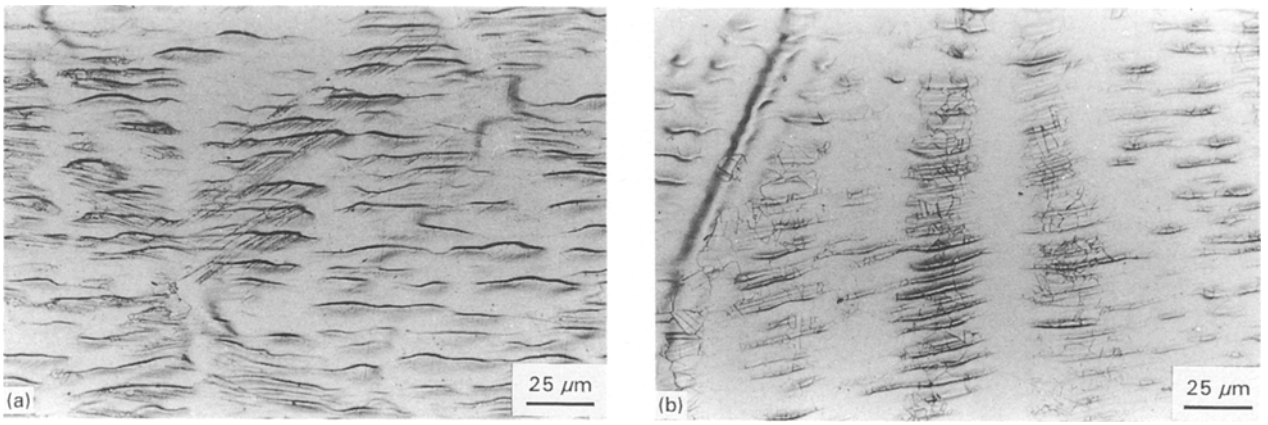

Figure 10 The effect of temperature on the microstructure at $\dot{\varepsilon} = 0.01\ s^{-1}$ (a) 900 °C, (b) 1200 °C.

Fig. 9a than that of fast strain rate. The effect of temperature on the corresponding microstructures can be compared in Fig. 10a and b, which deformed at a strain rate of $0.01\ s^{-1}$. More recrystallized grains are found at the high temperature of 1200 °C than at the low temperature of 900 °C.

4. Conclusions

The hot-working characteristics of as-cast Co–Ni–Cr–Mo ESR alloy were evaluated by hot tension and hot compression tests using a Gleeble-2000A simulator. The main results are as follows.

1. The optimum preheat temperature is 1250 °C, because it can improve the as-cast dendritic structure and result in good hot ductility of pre-heated alloy over a wide range of forging temperatures. The minimum working temperature is determined as 800 °C to ensure acceptable hot workability.

2. The drop-off of hot ductility at 1300 °C or higher temperature was due to the incipient melting of grain boundaries.

3. The flow stress of the alloy shows a strong dependence on the strain rate and temperature. The stress increases rapidly with increasing strain rate and decreasing temperature.

Acknowledgement

The authors thank the Ministry of Economic Affairs, Taiwan, for financially supporting this research project.

References

1. G. D. SMITH, U S Pat. 3356 542 (1976).
2. J. S. SLANEY, U S Pat. 3767 385 (1973).
3. J. S. SLANEY and R. A. NEIBIDO, *Mettalogr.* **16** (1983) 137.
4. F. C. HAGON, H. W. ANTES, M. D. BOLDG and J. S. SLANEY, "Superalloy 1984" (TMS-AIME, Warrendale, PA, 1984) p. 623.
5. M. LORENZ, M. SEMLTITISH, B. PANIC, H. WEBER and H. G. WILLERT, *Eng. Med.* **7** (1978) 241.
6. R. T. HOLT and W. WALLACE, Mechanical Engineering Report, MS-143 (National Research Council Canada, Ottawa, 1980).
7. T. C. TISONE, *Acta Metall.* **21** (1973) 229.
8. J-P. IMMARIGEON, K. RAJAN and W. WALLACE, *Metall. Trans. A* **15** (1984) 339.
9. G. L. FITZSIMONS, PhD thesis, University of Pittsburgh (1980).
10. R. P. SINGH and R. D. DOHERTY, *Metall. Trans. A* **23** (1992) 307.
11. M. J. DONACHIE, JR, in "Metal Handbook", Desk Edition, edited by H. E. Boyer and T. L. Gall (ASM, Metals Park, OH, 1985) p. 16.5.
12. R. E. BAILEY, *Metal. Eng. Q.* **5** (1975) 43.
13. A. H. GRAHAM and J. L. YOUNGBLOOD, *Metall. Trans.* **1** (1970) 423.
14. M. RAGHAVAN and B. J. BERKOWITZ, *Scripta Metall.* **14** (1980) 1009.
15. M. RAGHAVAN, B. J. BERKOWITZ and R. D. KANE, *Metall. Trans. A* **11** (1980) 203.
16. J. M. DRAPIER, P. VIATOUR, D. COUTSOURADIS and L. HABRAKEN, *Cobalt* **49** (1970) 171.
17. R. P. SINGH and R. D. DOHERTY, *Metall. Trans. A* **23** (1992) 321.
18. G. E. DIETER, "Workability Testing Techniques" (ASM, Metals Park, OH, 1984) p. 73.
19. R. PILKINGTON, C. W. WILLOUGHBY and J. BARFORD, *Metal Sci. J.* **5** (1971) 1.
20. B. WEISS, G. E. GROTKE and R. STICKLER, *Weld. J.* **10** (1970) 471.
21. H. G. SUZUKI, H. FUJII, N. TAKANO and K. KAKN, *Indust. Heat* Vol. LV, **10** October (1988) 18.
22. J. C. TASI and J. B. DUH, *Scripta Metall.* **27** (1992).
23. T. NAKAMURA, M. UEKI and S. HORIE, *J. Jpn Inst. Light Metals* **25** (1975) 81.
24. K. P. RAO and Y. V. R. K. PRASAD, *J. Mech. Working Technol.* **13** (1986) 83.
25. D. A. HUGHES and W. D. NIX, *Metall. Trans. A* **19** (1988) 3013.
26. M. UEKI, S. HORIE and T. NAKAMURA, *J. Mech. Working Technol.* **11** (1985) 355.
27. S. L. SEMIATIN, N. FREY, S. M. EL-SOUDANI and J. D. BRYANT, *Metall. Trans. A* **23** (1992) 1719.
28. H. J. McQUEEN and J. J. JONAS, in "Plastic Deformation of Materials, Treatise on Materials Science and Technology", Vol. 6, edited by R. J. Arsenault (Academic Press, New York, NY, 1975) p. 393.

Received 1 October 1992
and accepted 19 January 1994